International Forum on Aeroelasticity and Structural Dynamics
IFASD 2019
9-13 June 2019, Savannah, GA, USA

LIMIT CYCLE OSCILLATON PREDICTION FOR AIRCRAFT WITH EXTERNAL STORES – IFASD 2019

P.C. Chen[1], Z. Zhang[1], Z. Zhou[1], X.Q. Wang[2], and M.P. Mignolet[2]

[1]ZONA Technology, Inc.
9489 E. Ironwood Square Drive, Scottsdale, AZ 85258
pc@zonatech.com
zzc@zonatech.com
joe@zonatech.com

[2]SEMTE, Faculties of Mechanical and Aerospace Engineering,
Arizona State University, Tempe, AZ 85287-6106
xiaoquan.wang.1@asu.edu
marc.mignolet@asu.edu

Keywords: Nonlinear Aerodynamic and Nonlinear Structural Interaction, Aircraft with Stores, Limit Cycle Oscillation (LCO), Reduced Order Model, Nonlinear Structural Damping, Truly LCO Predictive Tool

Abstract: The objectives of this work is to develop a truly limit cycle oscillation (LCO) predictive tool in the Nonlinear Aerodynamic and Nonlinear Structural Interaction (NANSI) module of ZONA Euler Unsteady Solver (ZEUS). A novel Nonlinear Structural Damping (NSD) model has been developed that can be included in the NANSI module to provide the NSD effects for LCO prediction of aircraft with stores configurations. The NSD model requires a single parameter, γ, that needs to be estimated from the flight test data to quantify the nonlinear damping level. Based on the values of γ estimated from seven F-16 store configurations, it was found that γ is closely related to the flutter frequency of the F-16 with stores, by the "γ -estimator" equation. The flutter frequency of an eighth F-16 with stores configuration was first computed and the value of γ was determined using the γ -estimator so that it was not estimated by the flight test data. Using this value of γ in the NSD model to predict the LCO of the eighth F-16 with stores configuration at various flight conditions, a very good match with the corresponding flight test LCO measurements was obtained. Thus, the γ-estimator can be used for the LCO prediction prior to flight test of a new F-16 with stores configuration, rendering the NANSI module of ZEUS as a truly LCO predictive tool.

1 INTRODUCTION

Several current fighter aircraft with external store configurations persistently encounter Limit Cycle Oscillation (LCO) problems. LCO is a self-excited, sustained vibration of limited amplitude which can impact a pilot's control authority over the aircraft, ride quality, and weapon aiming. It can also induce structural fatigue and, under certain circumstances, flutter. Denegri [1] provided a detailed description of the aircraft/store LCO phenomenon. Norton [2] gave an excellent overview of LCO for a fighter aircraft carrying external stores and its sensitivity to store carriage configuration and mass properties. Because of this sensitivity, the LCO clearance of a modern fighter aircraft should be addressed for all possible store/weapon configurations. Given the drastic number of such configurations, this effort is a major engineering task in aircraft/store weapon compatibility certification. It requires accurate aeroelastic predictions within a short-time frame as demanded by rapid military responses when facing today's ever-changing international situation. Further, since there can be thousands of store/weapon

combinations for a typical fighter aircraft, the LCO predictions must also be computational efficient to rapidly identify the critical cases. A robust post-processing procedure is also needed to identify a wide variety of aeroelastic response characteristics including flutter, divergence and LCO.

It is generally believed that LCO of an aircraft with stores is a post flutter phenomenon that belongs to the so-called supercritical LCO mechanism. When the flight condition of the aircraft is beyond its flutter boundary, the aircraft's aeroelastic system is unstable and a divergent response of the structure occurs if the aeroelastic system is linear. However, if the aeroelastic system is nonlinear and includes a "LCO bounding mechanism" dependent on the amplitude of the structural response to the aeroelastic system, then the growth of the divergent response due to flutter can be limited resulting in LCO at a particular amplitude. The source of the LCO bounding mechanism, which could be from the aerodynamics, structure or both, still remains to be fully understood and is a long-standing research issue. Many researchers believe that the nonlinearity involved in the LCO bounding mechanism is solely induced by oscillating transonic shocks and/or shock induced flow separation. This type of approach for predicting LCO is defined herein as the sole nonlinear aerodynamic approach. If this is the correct bounding mechanism, the LCO can be predicted using high fidelity Computational Fluid Dynamics (CFD) tools coupled with a linear structural model. Using a CFD tool called the AERO-F/S Suite developed by Farhat [3], Pasiliao [4] performed an LCO study on an F-16 with stores configuration that experienced LCO during flight tests and found good correlation of the onset LCO Mach number (the flutter boundary) between the predicted and flight test measured results. This good matching results from the CFD code accurately capturing the transonic shock effects that normally lower the predicted flutter boundary in transonic flow regions as compared to that predicted by the linear unsteady aerodynamic methods such as the Doublet Lattice Method (DLM) and ZAERO [5].

However, even with this good transonic flutter predictive capability, Pasiliao's investigation failed to predict LCO. On this basis, it appears that the nonlinear aerodynamics provided by the CFD methodology alone is not sufficient as a predictive LCO tool. Another sole nonlinear aerodynamic approach was adopted by Prananta et al. [6] using the ENFLOW CFD system developed by the National Research Laboratory (NLR). It predicted LCO of an F-16 configuration with stores at Mach number (M) = 0.9 and angle of attack (AoA) = 7°. However, it is known from the flight observation that the F-16 LCO could occur at cruise angle of attack normally in the range of 2° to 3°. Therefore, it is highly possible that Prananta et al. simulated the oscillating dynamic loads due to wing buffet, but not LCO, on the F-16 at that moderate angle of attack. The strongest evidences to show that the nonlinear aerodynamics cannot be the sole LCO bounding mechanism is the flight test data of two F-16 with store configurations presented by Brignac, [7]. The first is an F-16 with tip launchers 16S200 at weapon stations 1 and 9 and AIM-7F missiles at weapon stations 3 and 7 that experienced LCO during flight test at Mach numbers ranging from M=0.9 to M=1.4. However, at M=1.4 the transonic shock is absent from the F-16 wing and therefore the LCO bounding mechanism at M=1.4 cannot be induced by the oscillating shock. The second is a Block 40 F-16 with AIM-9P missiles and LAU-129 launchers at weapon stations 1 and 9, LAU-129 launchers at weapon stations 2 and 8, MK-84 bombs at weapon stations 3 and 7, 370 gallon tanks at weapon stations 4 and 6 and a 300 gallon tank at weapon station 5. The Mach number where LCO begins for this F-16 configuration with stores is 0.6, which is far below the transonic Mach numbers; showing once again that the LCO bounding mechanism at M=0.6 cannot be the oscillating shock. Therefore, it can be stated that the sole nonlinear aerodynamic approach supported by a computational methodology cannot adequately address the LCO phenomenon thus far.

In 1998, Chen et al. proposed nonlinear structural damping (NSD) as an LCO bounding mechanism [8]. The original justification for the appearance of structural nonlinearity was rooted in friction. In this perspective, note first an aircraft with stores consists of many mechanical joints to connect structural components to each other, the stores with their respective pylon/launcher and the pylons/launchers to the wing. Further, the dry friction in each mechanical joint could provide a stabilizing nonlinear structural damping to the aeroelastic system. Indeed, when flutter starts and the structural oscillating amplitude is small, the resulting forces due to the low-amplitude oscillation of the joints also are small, smaller than the static friction limit; thus no slip takes place and the oscillating amplitude continues to increase due to flutter. When the amplitude of response becomes large enough, the forces in the mechanical joins are sufficient to induce slip and thus dissipation takes place through friction. Note that the various joints of the aircraft act in series and thus the occurrence of slip progresses as the amplitude of response increases. Thus, the nonlinear structural damping of the aeroelastic system increases gradually as the oscillating amplitude due to flutter increases. If the flutter mechanism is not explosive, the friction damping in the aeroelastic system (the LCO bounding mechanism) may equate the destabilizing energy introduced into it through aerodynamics and an LCO may result. This scenario also was assessed by Arizona State University (ASU) researchers, see [9-11]. Padmanabhan et al. [12] performed an extensive LCO investigation using computational fluid dynamics method by varying the stiffness and damping in the wing-store attachments and found that the nonlinear structure is likely to produce/contribute to the F-16 LCO. The existence of Coulomb friction in the F-16 structure at large amplitude oscillation also has been confirmed by the ground vibration test performed by Dossogne et al [13].

The NSD mechanism is not limited to friction, it can include other forms of damping and dissipation. In fact, Sharma and Denegri [14] performed a time integration of the nonlinear aeroelastic equations (TINA) that reads:

$$\left[M_{ij}\right]\left\{\ddot{q}_j\right\}+\left[D_{ij}(g)-\frac{1}{4k}\rho bVQ_{ij}^{i}\right]\left\{\dot{q}_j\right\}+\left[K_{ij}-\frac{1}{2}\rho V^2Q_{ij}^{r}\right]\left\{q_j\right\}=0 \tag{1}$$

Where M_{ij}, K_{ij}, and $D_{ij}(g)$ are the generalized stiffness, mass and damping matrices, respectively. ρ, b, V and q_j are the air density, reference chord, free stream velocity and generalized modal coordinates, respectively. Q_{ij}^{i} and Q_{ij}^{r} are the imaginary part and real part of the frequency-domain generalized aerodynamic forces that are pre-computed by the linear Doublet Lattice Method (DLM).

The NSD mechanism was modeled globally in Equation (1) through the generalized damping matrix $D_{ij}(g)$ which is defined as a prescribed, monotonically increasing nonlinear function of the structural acceleration, g, at a reference point. During the time-domain simulation, the generalized damping matrix is updated at each time step according to g. The TINA computed LCO amplitudes compared favorably with the flight test data of an F-16 with stores configuration; proving that the NSD mechanism is a strong contender as an LCO bounding mechanism. In this perspective, it is useful to recognize the parallel between Equation (1) and the classic one degree-of-freedom van der Pol equation of a mass (m), spring (k), linear damping (c), and nonlinear damping (α) system shown as follows:

$$m\,\ddot{q}+\left(\alpha q^2-c\right)\dot{q}+k\,q=0 \tag{2}$$

which is well known to exhibit LCO [15]. The similarity between Equations (1) and (2) is particularly clear if the unstable aerodynamic forces are modeled by the negative damping term $-c\dot{q}$ present in Equation (2).

However, because of the linear aerodynamics from DLM, the TINA computed onset LCO Mach numbers do not correlate very well with the flight test data. This is because the linear DLM cannot capture the transonic shock effects; thereby, its predicted flutter boundary which is the onset of the LCO condition is not accurate. The linear aerodynamic and nonlinear structural damping model in TINA is defined herein as the sole nonlinear structural approach.

The ideal computational methodology for predicting LCO is the combination of the sole nonlinear aerodynamic approach and the sole nonlinear structural approach. This calls for a Nonlinear Aerodynamic and Nonlinear Structural Interaction (NANSI) simulation tool that must have the following features: (1) the unsteady aerodynamic method must be nonlinear and able to capture transonic shocks, (2) flow viscosity should be included, (3) all components of the configuration, particularly the external stores, must be modeled both structurally and aerodynamically, and (4) structural nonlinearities can be modeled in the numerical simulation. In addition, the simulation tool must be computationally efficient so that results can be generated for a massive number of aircraft with stores configurations at various flight conditions with an affordable computational cost. One such a simulation tool is the NANSI module in ZONA's Euler Unsteady Solver (ZEUS).

2 ZEUS (ZONA'S EULER UNSTEADY SOLVER) WITH NANSI MODULE

ZEUS [16] is a ZONA Euler Unsteady Solver that integrates the essential disciplines required for aeroelastic design/analysis. It uses the Cartesian Euler flow solver with a boundary-layer option to include viscous effects as the underlying aerodynamic force generator coupled with structural modal solution to solve various aeroelastic problems, such as maneuver loads, store ejection loads, gust loads, static aeroelastic/trim and nonlinear flutter analysis. The structural modal solution can be directly imported from commercial structural finite element software.

ZEUS is driven by the need of higher fidelity CFD methods for aeroelastic analysis, yet the aerospace industry is still accustomed to using aerodynamic panel methods such as the doublet lattice method and ZAERO. This is because these methods utilize a paneling scheme, which is far simpler than the grid generation procedure required by the CFD methods. Towards this end, ZEUS has been developed to use the input format that is very similar to that of Nastran and ZAERO. In fact, the majority of the input data cards of ZEUS are nearly identical to those of ZAERO. ZEUS also is equipped with an automated mesh-generation scheme that can generate a volume mesh by automatically extending from a surface mesh. This automated mesh-generation greatly relieves users from the tedious CFD nesh generation procedure, and is one of the primary advantages of using ZEUS over other CFD codes. In addition, ZEUS has an overset mesh capability that can handle very complex aircraft configurations such as a complete aircraft with external stores, in which aircraft and stores are modeled by different blocks of mesh. The communication of the flow solution among the different blocks of mesh is handled through the interpolation of the flow solutions in the overlapped-mesh regions. Solution convergence is achieved by Newton sub-iterations. An F-16 with external stores configuration, known as the Typical-LCO configuration which encountered LCO during flight tests [1], is selected as the test case to demonstrate the overset mesh capability of ZEUS. The surface mesh represented by a panel model of this typical-LCO configuration is shown in Figure 1(a) where three underwing stores/missiles mounted under each side of the wing can be seen. To model such a complex configuration, we use 24 blocks of mesh whose 3-D view, X-Y view and Y-Z

view are shown in Figures 1(b), 1(c), and 1(d), respectively, rendering an overset mesh for the ZEUS computation.

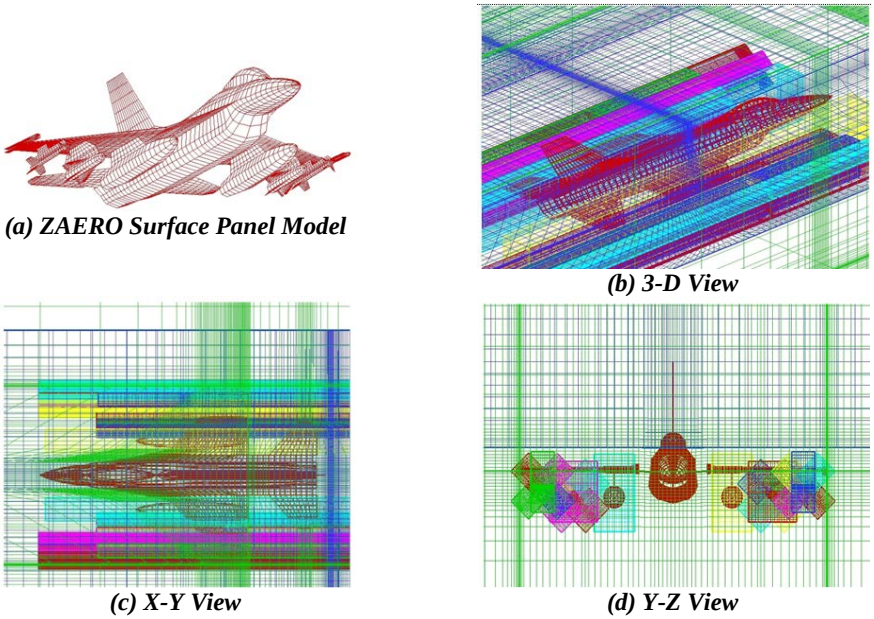

(a) ZAERO Surface Panel Model

(b) 3-D View

(c) X-Y View

(d) Y-Z View

Figure 1: Overset mesh to model the F-16 Typical-LCO configuration.

Because the overset mesh scheme allows the ease of modeling complex configurations, ZEUS is an ideal aerodynamic solver for NANSI simulation of massive number of aircraft with stores configurations. If a wide range of store aerodynamic models can be pre-established and saved on a weapons database, a ZEUS aerodynamic model of a given aircraft with stores can be easily obtained by simply retrieving the store aerodynamic models from the weapons database and including these models in the clean wing aerodynamic model, rendering an overset mesh that can accurately account for the aerodynamic interference between aircraft and stores.

The NANSI module in ZEUS essentially solves the following nonlinear aeroelastic equation of motion:

$$M_{ij}\ddot{q}_j + \left[D_{ij} + D^{(2)}_{ijl} q_l + D^{(3)}_{ijlp} q_l q_p \right] \dot{q}_j + [K_{ij} + K^{(2)}_{ijl} q_l + K^{(3)}_{ijlp} q_l q_p] q_j = F_i(q_j, \dot{q}_j) \tag{3}$$

where $D^{(2)}_{ijl}$ and $D^{(3)}_{ijlp}$ are quadratic and cubic nonlinear structural damping coefficients, respectively. $K^{(2)}_{ijl}$ and $K^{(3)}_{ijlp}$ are quadratic and cubic nonlinear structural stiffness coefficients, respectively. $F_i(q_j, \dot{q}_j)$ are the generalized aerodynamic forces provided by the ZEUS' Euler solver with viscous effects.

Note that Equation (3) includes both nonlinear damping and nonlinear stiffness terms. Since the wing tip LCO amplitudes of various F-16 with stores configurations that we have observed from their flight test data so far are all less than one inch, we ignore these nonlinear stiffness terms in Eq. (3). This is because such a small LCO amplitude is far less than the threshold of 15% of wing span below which the nonlinear stiffness terms are typically insignificant, However, we will verify this assumption in a latter section. Excluding the nonlinear stiffness terms, Equation (3) becomes:

$$M_{ij}\ddot{q}_j + \left[D_{ij} + D^{(2)}_{ijl} q_l + D^{(3)}_{ijlp} q_l q_p \right] \dot{q}_j + K_{ij}\, q_j = F_i(q_j, \dot{q}_j) \tag{4}$$

It should be noted that the model of Equation (4) is a *generalized van der Pol* model, i.e. a natural extension of the classic van der Pol equation of Equation (2) to a multi-degree-of-freedom system. Given the well-known LCO features of the classic van der Pol equation, it is surmised that Equation (4) can indeed exhibit the capability to curb the increasing structural response post flutter and lead to LCO. The coefficients, $D_{ijl}^{(2)}$ and $D_{ijlp}^{(3)}$, can be identified from the structural finite element model using a Reduced Order Modeling (ROM) technique developed by the Arizona State University (ASU) group [17-19].

3 DEVELOPMENT OF AN NSD MODEL: THE GENERALIZED VAN DER POL MODEL

Since the global NSD mechanism to be modeled arises when the amplitude of the motions becomes "large enough", an appropriate framework for its formulation is finite deformation viscoelasticity in which the response is further expressed as a superposition of the linear structural modes. Then, this effort is effectively the extension to viscoelasticity of the nonlinear reduced order modeling of elastic structures developed by the ASU group. This extension can be carried out by replacing the *elastic* constitutive relation (Hooke's law) by a *viscoelastic* one. Here, we adopt a simple Maxwell [20] viscoelastic model. That is, the stress tensor $\boldsymbol{S}$ of components S_{ij} will be expressed in terms of its strain counterparts E_{ij} as (summation over repeated indices implied):

$$S_{ij} = C_{ijkl}\, E_{kl} + D_{ijkl}\, \dot{E}_{kl} \tag{5}$$

where C_{ijkl} denotes the fourth order elasticity tensor and D_{ijkl} is a *dissipation tensor* relating the stress to the strain rate. Under the model of Eq. (5), the power dissipated in the infinitesimal element considered is

$$P_{dissip} = \dot{E}_{ij} S_{ij} = \dot{E}_{ij} D_{ijkl}\, \dot{E}_{kl} \tag{6}$$

which will be positive at all times and for all elements if D_{ijkl} is positive definite. A simple choice of a tensor with this property [20] is

$$D_{ijkl} = \lambda_d\, \delta_{ij}\, \delta_{kl} + \mu_d \left(\delta_{ik}\, \delta_{jl} + \delta_{il}\, \delta_{jk}\right) \tag{7}$$

where δ_{ij} is the Kronecker delta ($\delta_{ij} = 1$ if $i = j$, 0 otherwise) and λ_d and μ_d are parameters. The positive definiteness of D_{ijkl} is guaranteed when λ_d and μ_d are both positive. Continuing the analogy with this tensor, one can also define a dissipation modulus E_d and ratio ν_d (similar to the Young's modulus and Poisson's ratio) through the transformation:

$$\mu_d = \frac{E_d}{2\left(1+\nu_d\right)} \quad \text{and} \quad \lambda_d = \frac{E_d\, \nu_d}{\left(1+\nu_d\right)\left(1-2\nu_d\right)} \tag{8}$$

Adopting the dissipation model of Equation (7) leads to a 2-parameter model, i.e., with either λ_d and μ_d or E_d and ν_d characterizing it. It remains to address the estimation of the nonlinear damping parameters $D_{ijl}^{(2)}$ and $D_{ijlp}^{(3)}$. For a particular set of values of the parameters E_d and ν_d of Equation (8), the parameters $D_{ijl}^{(2)}$ and $D_{ijlp}^{(3)}$ can be determined from a commercial finite element model of the wing/aircraft by following the same procedure as the one for the estimation of the nonlinear stiffness terms $K_{ijl}^{(2)}$ and $K_{ijlp}^{(3)}$ in the ASU nonlinear structural reduced order modeling approach [17-19]. Further, the damping parameters $D_{ijl}^{(2)}$ and $D_{ijlp}^{(3)}$ can be seen

to *depend linearly* on λ_d and μ_d. Thus, estimating the NSD, $D_{ijl}^{(2)}$ and $D_{ijlp}^{(3)}$, for two sets of values of E_d and ν_d will permit the interpolation or extrapolation of the damping parameters to other values of E_d and ν_d that can be identified from a commercial finite element model of the aircraft.

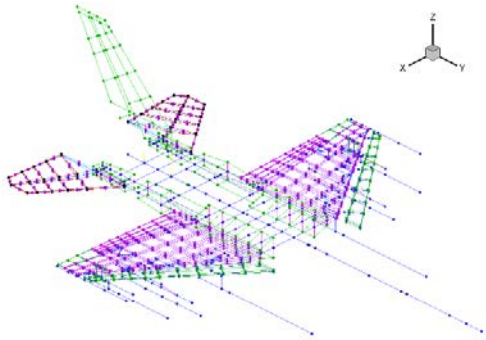

Figure 2: Finite Element Model of the F-16 Typical LCO Configuration.

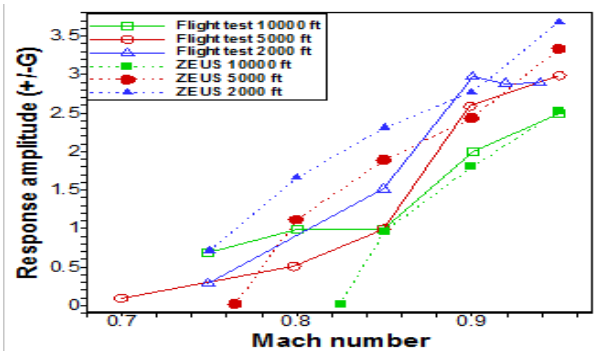

Figure 3: LCO Amplitudes of the F-16 Typical-LCO Configuration.

Using the structural finite element model (FEM) of the F-16 Typical LCO configuration shown in Figure 2 to identify E_d and ν_d and subsequently applying the NANSI module to compute the LCO responses, the authors [21] found that the ratio ν_d has insignificant effect on the LCO amplitude. Thus, only the elemental dissipation modulus E_d with a tunable parameter γ needs to be determined by minimizing the differences between the flight-test measured LCO amplitude and the corresponding NANSI prediction at one flight condition. Since the structural characteristics of the aircraft are independent of the flight condition, the coefficients $D_{ijl}^{(2)}$ and $D_{ijlp}^{(3)}$ can be applied to other flight conditions. Applying this technique to the F-16 Typical LCO configuration at M=0.9 and altitude (h)=5 kft, the authors determined γ=0.682×10^{-4} and subsequently computed the LCO amplitudes at various flight conditions. Good correlation between the NANSI predictions and flight test data was obtained as the one shown in Figure 3.

The authors also computed the accelerations (G's) at wing tip of the F-16 Typical LCO configuration at various Mach numbers and altitude=5 kft without the NSD and compared to those with the NSD. The comparison of the time histories between these two sets of responses is shown in Figure 4. Without the NSD model, the results computed by ZEUS at Mach numbers above 0.75 are all divergent responses, i.e. flutter. Once again, this verifies that the nonlinear aerodynamic effects alone are not sufficient to induce LCO. On the other hand, the NSD effects incorporated in the NANSI module of ZEUS can bound the divergent response due to flutter, resulting LCO. Note that the LCO frequencies of the F-16 Typical LCO configuration predicted by the NANSI module of ZEUS with and without the NSD models are all around 8.3 Hz which are in good agreement with the flight test frequency of 8.0 Hz. This suggests that the flutter frequency (ω_f) computed by ZEUS without the NSD can be used to predict the LCO frequency prior to the flight test.

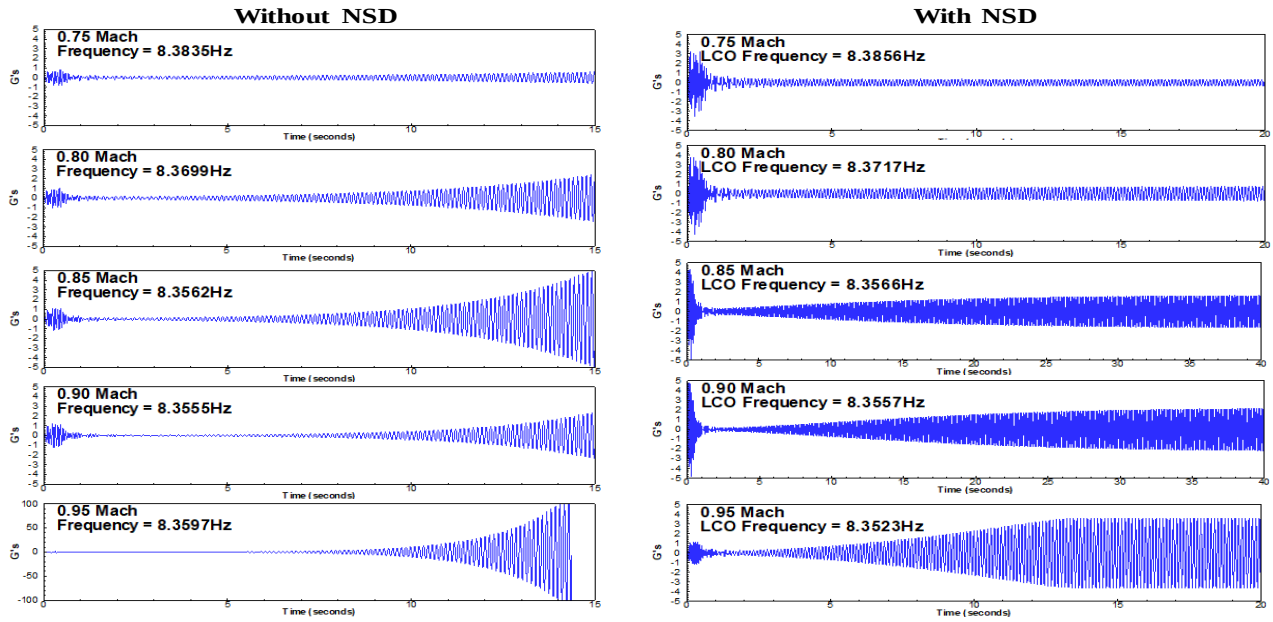

Figure 4: Comparison of responses of the F-16 Typical LCO configuration with and without the NSD

4 ASSESSMENT OF NONLINEAR STIFFNESS EFFECTS ON LCO

The ROM technique developed by the ASU group [17-19] also can be applied to the FEM of the F-16 Typical LCO configuration to identify its nonlinear stiffness coefficients, $K_{ijl}^{(2)}$ and $K_{ijlp}^{(3)}$, in Equation (3). Shown in Figure 5 is a comparison of the wing tip acceleration time histories computed by the NANSI module of ZEUS with and without nonlinear stiffness effects for a linear damping model at M=0.85 and h=5 kft. Comparing the nonlinear response to the linear response, noticeable nonlinear stiffness effects can be seen only after the acceleration growing beyond 20 G's. The LCO bounding mechanism provided by the nonlinear stiffness can limit the divergent response due to flutter at 90 G's only after which an LCO is fully developed. It should be noted that the F-16 flight test mission abort criteria established by the U.S. Air Force only allows the maximum G below a 5-G level which is far less than 90 G's. Based on this study, it is concluded that the nonlinear stiffness is not a viable LCO bounding mechanism for the F-16 with stores configurations. This is also confirmed by Northington and Pasiliao [22] whose experiments showed no stiffness nonlinearity in the F-16 wing alone. Thus, for the following F-16 with stores configurations the nonlinear stiffness terms are excluded from Equation (3) and the NANSI module of ZEUS only solves Equation (4).

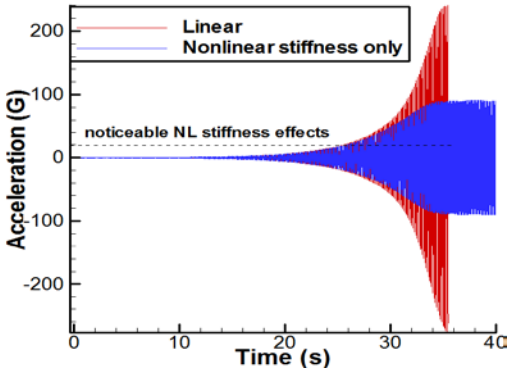

Figure 5: Comparison of tip acceleration time histories of the F-16 typical LCO configuration computed by the NANSI module with and without nonlinear stiffness.

5 APPLICATIONS OF NANSI MODULE TO OTHER F-16 WITH STORES CONFIGURATIONS.

In addition to the F-16 Typical LCO configuration (denoted as LCO No. 1 in Table 1), we also have applied the NANSI module of ZEUS with the NSD model and without the nonlinear stiffness effects to other six F-16 with stores configurations, denoted as LCO No. 2 (Non-Typical LCO A), LCO No. 3 (Non-Typical LCO B), LCO No. 4 (Denegri), LCO No. 5 (SL2 Fin-on), LCO No. 6 (SL2 Fin-off), and LCO No. 7 (SL3 Fin-on), shown in Table 1 along with

their associated store types and weapon-station locations as well as flutter/LCO frequencies and the values of γ.

Table 1: Seven F-16 with stores configurations investigated.

LCO No.	Name	Weapon Station 1	Weapon Station 2	Weapon Station 3	Weapon Station 4	Weapon Station 5	ω_f (Hz)	γ (s)
1	Typical LCO	LAU-129	LAU-129 AIM-9P	Air-to-ground Missile A	Empty 370 Gal Tank	300 Gal Tank	8.3	0.682×10^{-4}
2	Non-Typical LCO A	LAU-129 AIM-120	LAU-129 AIM-9P	Guided Bomb	Full 370 Gal Tank	300 Gal Tank	4.4	$11.7.\times10^{-4}$
3	Non-Typical LCO B	LAU-129	LAU-129 AIM-120	General purpose Bomb	¼-full 370 Gal Tank-	300 Gal Tank	7.0	1.9×10^{-4}
4	Denegri	LAU-129 AIM-9L	LAU-120 AIM-9L	Air-to-ground Missile B	Half-full 370 Gal Tank	300 Gal Tank	5.0	4.316×10^{-4}
5	SL2 Fin-on	LAU-129 Dummy Missile with Fin-on	LAU-129 AIM-9L	LAU-118 CATM-88	Half-full 370 Gal Tank	300 Gal Tank	5.2	1.284×10^{-4}
6	SL2 Fin-off	LAU-129 Dummy Missile with Fin-off	LAU-129 AIM-9L	LAU-118 CATM-88	Half-full 370 Gal Tank	300 Gal Tank	5.17	1.30×10^{-4}
7	SL3 Fin-on	LAU-129 Dummy Missile with Fin-on	Empty	MK-84	Half-full 370 Gal Tank	Empty	5.3	2.203×10^{-4}

Figure 6.(a) presents the ZEUS surface mesh of the F-16 non-typical LCO A configuration [1] (denoted as LCO No. 2 in Table 1). The comparison of LCO amplitudes between the flight test data and ZEUS computed results is shown in Figure 6.(b). The parameter γ=11.7×10^{-4} for this case is tuned by the flight test data at M=0.95 and h=5 kft. The flight test data shows that LCO occurs only within a narrow Mach number region and disappears at Mach number above 0.98. This trend is well captured by the NANSI module of ZEUS.

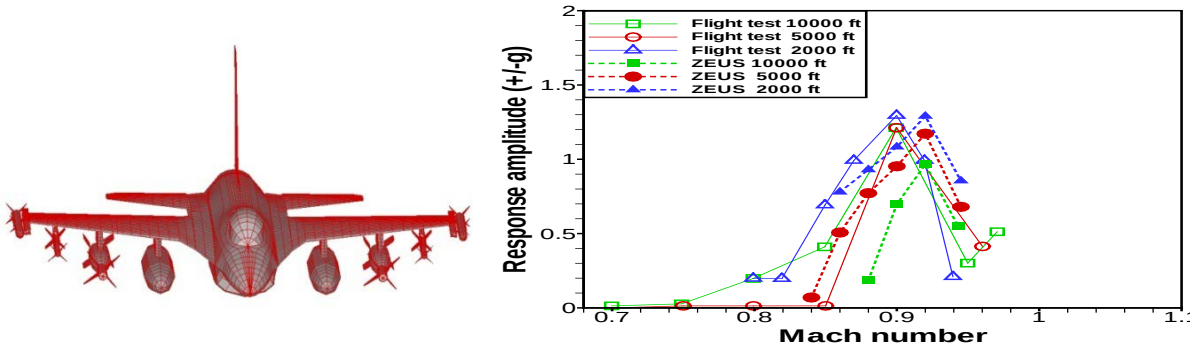

(a) **ZEUS Surface Mesh**

(b) **Comparison between NANSI predicted LCO Amplitudes and Flight Test Data**

Figure 6: The F-16 non-typical LCO A configuration.

The flight test data and stores carried by the F-16 non-typical LCO B (denoted as LCO No. 3 in Table 1) and the F-16 Denegri (denoted as LCO No. 4 in Table 1) configurations can be

found in [23]. The ZEUS surface meshes and the comparisons of the NANSI predicted LCO amplitudes with the flight test data of these two configurations are presented in Figures 7 and 8, respectively. The parameter γ of the F-16 non-typical LOC B configuration is tuned based on the flight test data at M =0.9 and h=5 kft and found to be $\gamma = 1.9 \times 10^{-4}$. The parameter γ of the F-16 Denegri configuration is similarly tuned based on the flight test data at M =0.90 and h=2 kft and found to be $\gamma = 4.316 \times 10^{-4}$. For the F-16 non-typical LCO B configuration, ZEUS under-predicts the LCO onset Mach number but the overall shape of the LCO amplitudes correlates reasonably well with the flight test data. The LCO onset Mach number of the F-16 Denegri configuration predicted by ZEUS agrees well with that of the flight test data but ZEUS slightly under-predicts the maximum LCO amplitude.

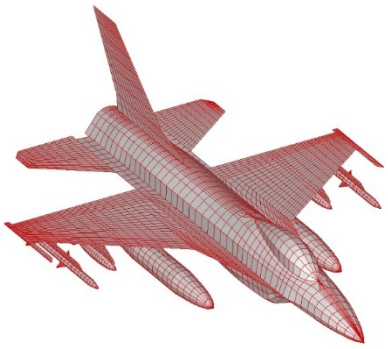

(a) ZEUS Surface Model

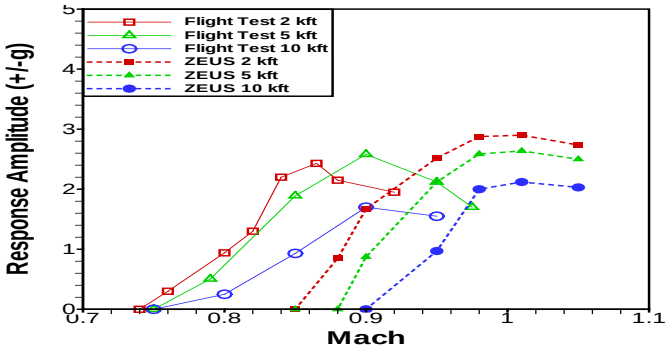

(b) Comparison between NANSI predicted LCO Amplitudes and Flight Test Data

Figure 7: The F-16 non-typical LCO B configuration.

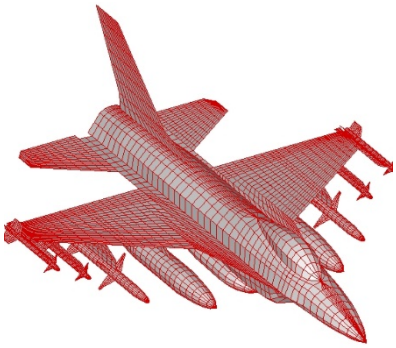

(a) ZEUS Surface Model

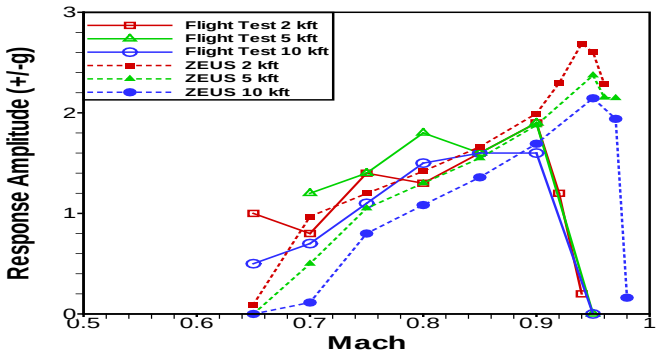

(b) Comparison between NANSI Predicted LCO Amplitudes and Flight Test Data

Figure 8. The F-16 Denegri configuration.

The F-16 SL2 configuration carries the AIM-9 dummy missiles on the wing tips. Two types of dummy missiles shown in Figure 9 were fabricated, the first one with control surface fins on (denoted as LCO No. 5 in Table 1) while the second with control surface fins off (denoted as LCO No. 6 in Table 1) but with balance weight to match the weight of the first type so that the mass distributions between these two configurations are identical. The only difference between these two configurations is that aerodynamic forces generated by the fin-on configuration whereas the fin-off configuration cannot. Flight tests of the SL2 configurations were performed by Major Masset in Sept. 2010 at Edwards Air Force Base (AFB) and supported by Air Force SEEK EAGLE Office (AFSEO) to study the impact of the fin aerodynamics on the LCO amplitudes at various Mach number and altitudes. The flight test data was documented in Major Masset's thesis [24].

(a) with Control Surface **(b) without Control Surface.**

Figure 9: Dummy AIM-9 missiles.

The ZEUS surface meshes and the comparisons of the NANSI predicted LCO amplitudes with the flight test data of the F-16 SL2 with fin-on and fin-off configurations are presented in Figures 10 and 11, respectively. It should be noted that these two configurations also have been studied previously by the authors [25] using ZEUS. The parameter γ of the fin-on and fin-off configurations were found to be $\gamma = 1.284 \times 10^{-4}$ and $\gamma = 1.30 \times 10^{-4}$, respectively, which are approximately the same. This is expected because the structural characteristics of these two configurations are nearly the same, verifying that the parameter γ is a purely structural parameter and is independent of the flight condition. For both configurations, the ZEUS predicted LCO onset Mach numbers and LCO amplitudes agree well with the flight test data. Even with such a small area of missile fins, the impact of the aerodynamic forces generated by the fins on the LCO response is well captured by ZEUS.

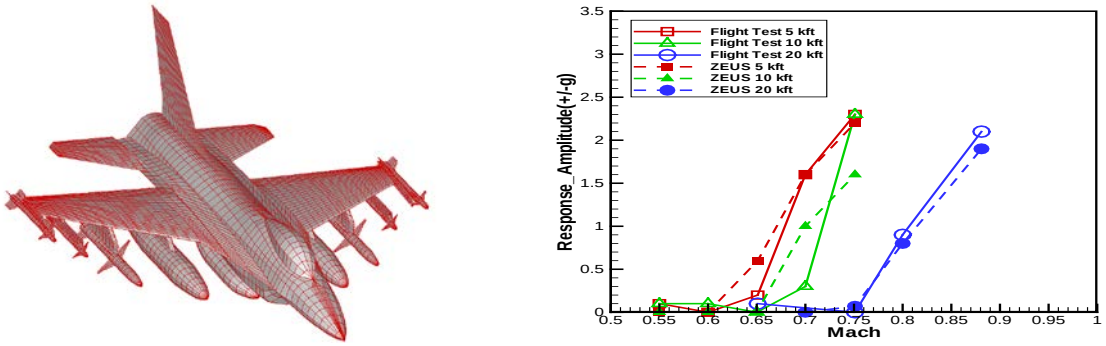

(a) ZEUS Surface Mesh **(b) Comparison between NANSI Predicted LCO Amplitudes and Flight Test Data**

Figure 10: The F-16 SL2 with fin-on configuration

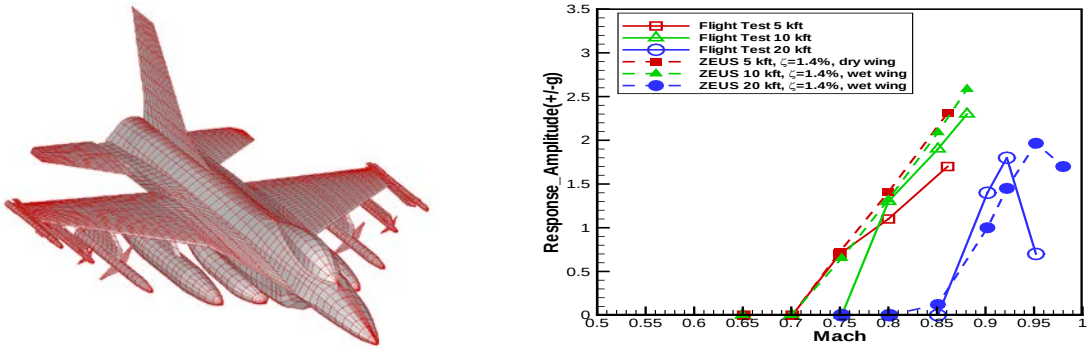

(a) ZEUS Surface mesh **(b) Comparison between NANSI Predicted LCO Amplitudes and Flight Test Data**

Figure 11: The F-16 SL2 with fin-off configuration.

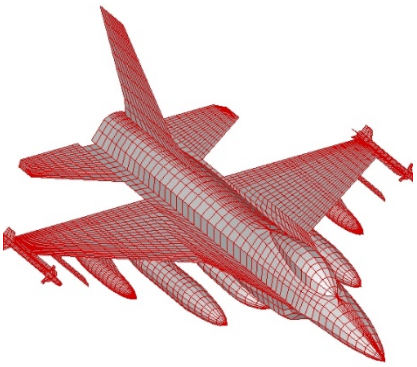

(a) ZEUS Surface Mesh

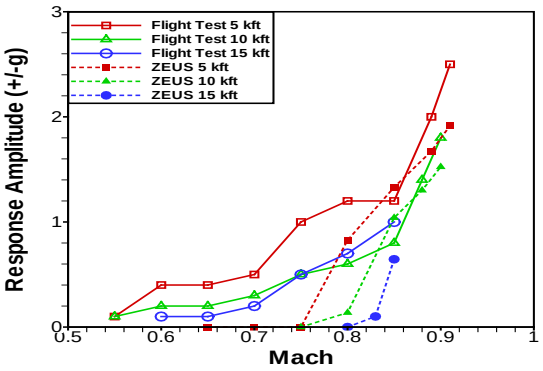

(b) Comparison between NANSI Predicted LCO Amplitudes and Flight Test Data

Figure 12: The F-16 SL3 with fin-on configuration

The F-16 SL3 with fin-on configuration (denoted as LCO No. 7 in Table 1) is similar to the F-16 SL2 with fin-on configuration, i.e. also carries two dummy missiles on the wing tips, except that the weapon stations 2 and 8 are empty, weapon stations 3 and 7 carry MK-84 bomb, and weapon station 5 is empty. Flight tests of the F-16 SL3 configurations were also performed by Major Masset in Sept. 2010 at Edwards AFB and supported by AFSEO [24]. The ZEUS surface mesh and the comparison of the NANSI predicted LCO amplitudes with the flight test data of the F-16 SL3 with fin-on configurations are presented in Figures 12. The parameter γ of the F-16 SL3 with fin-on configuration is tuned based on the flight test data at M = 0.91 and *h*=5 kft and found to be $\gamma = 2.203 \times 10^{-4}$. ZEUS over-predicts the LCO onset Mach numbers but the maximum LCO amplitudes predicted by ZEUS correlates well with the flight test data. Major Masset also performed a flight test for the F-16 SL3 with fin-off configuration [24]. The F-16 SL3 with fin-off configuration is defined herein as the LCO No. 8 configuration whose flight test data will be used to validate the truly LCO predictive tool that will be discussed in a later section

6 ESTABLISHMENT OF A DATABASE OF NONLINEAR STRUCTURAL DAMPING PARAMETERS

So far, we have identified NSD models and tuned their respective parameter γ of six F-16 with stores configurations, namely the F-16 typical LCO, non-typical LCO A, non-typical LCO B, Denegri, SL2 with fin-on and fin-off as well as SL3 with fin-on configurations. Note that the F-16 SL2 with fin-off configuration shares the same NSD model as the SL2 with fin-on configuration. Incorporating these NSD modes in the NANSI module, we have obtained good correlation between the ZEUS predicted LCO amplitudes and the flight test data of these seven F-16 with stores configurations presented in Table 1.

For these six configurations, we have also tuned their respective parameters γ based on the flight-test measured LCO amplitudes at other two flight conditions. Therefore, for each configuration three spread values of γ are obtained. These three values of each configuration are shown on the vertical axis of Figure 13 of which the *x* axis is the flutter/LCO frequencies (ω_f) of these six configurations.

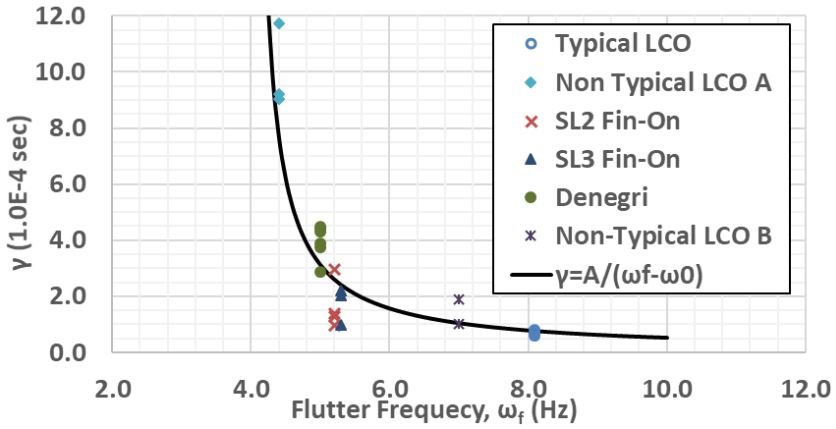

Figure 13: Correlation of the parameter γ as a function of the flutter/LCO frequency for six F-16 stores configurations.

The spread of these three values of γ for each F-16 with stores configuration shows the variation of the estimated parameter γ due to the uncertainty of the flight test data. Per Dr. Denegri of AFSEO who has been conducting flight tests of the F-16 with stores configurations since over thirty years ago, 10-20% variations of the LCO amplitudes may be fully expected on the same F-16 with stores configuration. Moreover, different LCO behaviors may occasionally be observed for similar configurations.

Performing a least square fit through the values of γ as a function of the flutter/LCO frequency, it is found that the following equation gives the best fit between γ and ω_f (the black line in Figure 13):

$$\gamma = \frac{\pi \times 10^{-4}}{(\omega_f - \omega_0)} \tag{9}$$

In this equation, ω_0 is selected to be 4.0 Hz which is the lowest possible flutter/LCO frequency among all F-16 with stores configurations that we have observed so far. Hereinafter, Equation (9) is referred to as the "γ-estimator".

7 DEVELOPMENT OF A TRULY LCO PREDICTIVE TOOL

Because the LCO frequency is usually approximately the same as the flutter frequency, which can be predicted by ZEUS without the NSD and nonlinear stiffness models, one can first compute the flutter frequency and then use Equation 9 to estimate the parameter γ. To verify this approach, we employ the F-16 SL3 with fin-off configuration as the testbed that has been defined as the LCO No. 8 configuration in the previous section. Figure 14 shows the acceleration response of the F-16 SL3 with fin-off configuration at M=0.85 and altitude=5 kft computed by ZEUS without the NSD model which reveals the flutter frequency to be equal to 5.139 Hz.

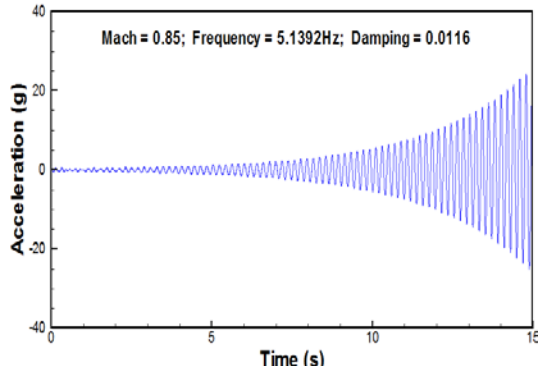

Figure 14: Acceleration response of the F-16 SL3 with fin-off configuration computed by ZEUS without NSD model.

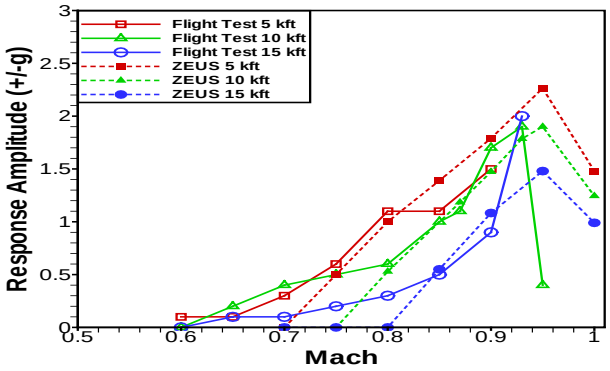

Figure 15: LCO amplitudes of the F-16 SL3 with fin-off configuration measured by flight test and computed by ZEUS

Using Equation (9), γ is estimated to be 2.75×10^{-4} which leads to the LCO predictions computed by the NANSI module of ZEUS with the NSD shown in Figure 15 as compared to the flight test data at various Mach numbers and altitudes. The good correlation between these two sets of results verifies that indeed using Equation (9) to estimate the parameter γ and then using the NANSI module in ZEUS to compute the LCO response is a viable approach for LCO prediction. Thus, this approach can be used for LCO prediction prior to flight test of a new F-16 with store configuration, rendering the NANSI module of ZEUS with the NSD model a truly LCO predictive tool.

8 CONCLUSIONS

The numerical prediction of the LCO amplitude of F-16 with stores has been the subject of an extensive number of investigations spanning approximately 3 decades but none of which has demonstrated a close matching between predicted and flight measured LCO amplitudes. The present investigation has however achieved this goal.

The distinguishing feature of our effort is the consideration of nonlinear structural damping that arises as part of nonlinear geometric effects induced by LCO. The implementation of this nonlinear structural damping within the ZEUS aeroelastic analysis framework necessitated the formulation of a nonlinear reduced order modeling strategy in which the structural motions are expressed as a linear combination of the linear modes of the aircraft with stores, and potentially additional modes. The resulting structural governing equations are found to exhibit linear and nonlinear damping terms in the form of a generalized van der Pol model.

Having established these governing equations, the second of our key breakthroughs is the determination of the nonlinear damping coefficients from a finite element model of the F-16 with stores exhibiting a specific viscoelastic behavior. Owing to the isotropic nature of the materials used in the F-16 and its stores, it is next argued that the dissipation tensor of their respective viscoelastic constitutive models is also isotropic and thus these dissipation tensors can be selected as proportional to the corresponding elastic tensors leaving a single tunable parameter, γ, to quantify the nonlinear damping level.

Damping characterization is a well-recognized challenge in structural dynamics especially for lightly damped structures in which several competing mechanisms, e.g., friction, material damping, exist and all of which have different behaviors. For these structures, there is no computational tool available to date to predict even the simplest measure of damping, i.e., the

linear damping ratio, let alone the nonlinear characteristics of damping. It is fully accepted in the community that small damping can only be estimated through a calibration process using test data. It is in this light that the present investigation relies on the calibration of the parameter, γ, but this is carried out only at a sole flight condition. Once calibrated, this NSD model is applied to all flight conditions and was observed to provide the correct trends of the LCO amplitude with Mach number and altitude as compared to flight test data.

An extensive validation analysis is next conducted on seven different F-16 with stores configurations for which flight test data is available. For each one, the parameter γ is selected so that the LCO amplitude predicted by ZEUS with NSD, i.e., the NANSI module, matched the flight test data at one altitude and one Mach number. Then, the NANSI module of ZEUS is used to predict the LCO amplitudes at other flight conditions and it is found that these results generally match well to very well with the flight test measurements. This effort thus successfully validates the NSD model and its NANSI implementation for the F-16 with stores LCO prediction.

A truly LCO predictive capability however would require that the value of γ can be obtained directly from a new aircraft with stores configuration prior to its flight test. This goal also has been achieved by investigating relationships between the value of γ and easily determined parameters that characterize the aeroelastic system. In that effort, we have demonstrated that γ is closely related to the flutter frequency of the F-16 with stores, by the "γ-estimator" equation. A validation of this relation as a fully independent predictor of the LCO amplitude has been carried out on an eighth F-16 with stores configuration for which the flutter frequency is first computed using ZEUS without the NSD. Using the γ–estimator, the value of this parameter is determined and is used in the NSD model to predict the LCO at various flight conditions. A very good match with the corresponding flight test LCO measurements of the eighth F-16 with stores configuration is obtained; verifying that the NANSI module of ZEUS with the γ–estimator can be a truly LCO predictive tool for aircraft with stores configurations.

9 ACKNOWLEDGEMENTS

This work was sponsored by the Air Force Office of Scientific Research under the Small Business Technology Transfer Research program (Contract Number: FA9550-16-C-0027). The contract monitor was Dr. Michael Kendra. The authors would like to thank Dr. Charles Denegri of the Air Force SEEK EAGLE Office for his valuable suggestions throughout the period of this project.

10 REFERENCES

[1] Denegri Jr., C.M., "Limit Cycle Oscillation Flight Test Results of a Fighter with External Stores," *Journal of Aircraft*, Vol. 37, No. 5, Sept.-Oct. 2000.

[2] Norton, W.J., "Limit Cycle Oscillation and Flight Flutter Testing," *Proceeds of the 21st Annual Symposium, Society of Flight Test Engineers*, Lancaster, CA, 1990, pp. 3.4-3.4-12.

[3] Farhat, C., Geuzaine, P., and Brown, G., "Application of a Three-Field Nonlinear Fluid-Structure Formulation to the Prediction of the Aeroelastic Parameters of an F-16 Fighter," *Computers and Fluids*, Vol. 32, No. 1, 2003, pp. 3-29.

[4] Pasiliao, C. L., "Characterization of Aero-Structural Interaction Flow-Field Physics," *Aerospace Flutter and Dynamics Council Fall Meeting*. Shalimar, FL. 25-26 October 2012.

[5] Chen, P.C., Lee, H.W., and Liu, D.D., "Unsteady Subsonic Aerodynamics for Bodied and Wings with External Stores Including Wake Effects", *Journal of Aircraft*, Vol. 30, No. 5, Sep-Oct. 1993. pp 168-628.

[6] Parananta, B.B., Kok, J.C., Spekreijse, S.P. Hounjet, M.H.L., and Meijer, J.J., "Simulation of Limit Cycle Oscillation of Fighter Aircraft at Moderate Angle of Attack," NLR-TP-2003-526, October 2003.

[7] Brignac W.J., "Limit Cycle Oscillation F-16 Experience,", *Aerospace Flutter and Dynamics Council Fall*. 10-11 May, 1989.

[8] Chen, P.C., Sarhaddi, D., and Liu, D.D., "Limit Cycle Oscillation Studies of a Fighter with External Stores," AIAA 98-1727, AIAA, 1998.

[9] Choi, G.G., Agelastos, A.M, Mignolet, M.P., and Liu, D.D., "On the Impact of Internal Friction on Flutter Onset and Limit Cycle Oscillations Amplitude," *International Forum on Aeroelasticity and Structural Dynamics 2005*, Munich, Germany, Jun. 28-Jul. 1, 2005.

[10] Kingsbury, D.W., Agelastos, A.M., Dietz, G., Mignolet, M.P., Liu, D.D., and Schewe, G., "Limit Cycle Oscillations of Aeroelastic Systems with Internal Friction in the Transonic Domain - Experimental Results," *Proceedings of the 46th Structures, Structural Dynamics, and Materials Conference*, Austin, Texas, Apr. 18-21, 2005. AIAA Paper AIAA-2005-1914.

[11] Choi, G.G., Agelastos, A.M., Mignolet, M.P., and Liu, D.D., "Effects of Internal Friction on the Dynamic Behavior of Aeroelastic Systems," *Proceedings of the 45th Structures, Structural Dynamics, and Materials Conference*, Palm Springs, California, Apr. 19-22, 2004. Paper AIAA-2004-1591.

[12] Padmanabhan, M.A., Dowell, E.H., Thomas, J.P., and Pasiliao, C. L., "Store-Induced Limit-Cycle Oscillations due to Nonlinear Wing-Store Attachment," *Journal of Aircraft*, Vol. 53, No. 3, May-June 2016.

[13] Dossogne, T, Noe'l, J.P., Grappasonni, C., Kerschen, G., Peeter, B., Debille, J. Vaes, M. and Schoukems, J., "Nonlinear Ground Vibration Identification of an F-16 Aircraft - Part II: Understanding Nonlinear Behaviour in Aerospace Structure Using Sine-Sweep Testing," *Proceedings of the International Forum on Aeroelasticity and Structural Dynamics Society*, Saint Petersburg, 2015, IFASD-2015-035.

[14] Sharma, V.K., and Dengeri, C.M., "Time Domain Aeroelastic Solution Using Exact Aerodynamic Influence Coefficients and Nonlinear Damping," *Proceedings of the International Forum on Aeroelasticity and Structural Dynamics Society*, London, 2013, IFASD-2013-29D. Royal Aeronautical Society, London, 2013, IFASD-2013-29D.

[15] Nayfeh, A.H., and Mook, D.T., *Nonlinear Oscillations*, Wiley 1979.

[16] Chen, P.C., Zhang, Z., Sengupta, A., and Liu, D., "Overset Euler/Boundary-Layer Solver with Panel-Based Aerodynamics Modeling for Aeroelastic Applications". *Journal of Aircraft*, 2009. 46(6): p. 2054-2068.

[17] Kim, K., Radu, A.G., Wang, X.Q., and Mignolet, M.P., "Nonlinear Reduced Order Modeling of Isotropic and Functionally Graded Plates," *International Journal of Non-Linear Mechanics*, Vol. 49, pp. 100-110, 2013.

[18] Perez, R.A., Wang, X.Q., and Mignolet, M.P., "Non-Intrusive Structural Dynamic Reduced Order Modeling for Large Deformations: Enhancements for Complex Structures," *Journal of Computational and Nonlinear Dynamics*, Vol. 9, No. 3, pp. 031008-1 - 031008-12, 2014.

[19] Mignolet, M.P., Przekop, A., Rizzi, S.A, and Spottswood, S.M., "A Review of Indirect/Non-Intrusive Reduced Order Modeling of Nonlinear Geometric Structures," Invited Paper, *Journal of Sound and Vibration*, Vol. 332, No. 10, pp. 2437-2460, 2013.

[20] Fung, Y. C., and Tong, P., Classical and Computational Solid Mechanics, World Scientific, River Edge, New Jersey, 2001.

[21] Zhang, Z., Chen, P. C., Wang X. Q., and Mignolet, p., "Nonlinear Aerodynamics and Nonlinear Structures Interaction for F-16 Limit Cycle Oscillation Prediction," *15th Dynamics Specialists Conference*, AIAA SciTech Forum, AIAA-2016-1796.
[22] Northington, J.S. and Pasiliao, C.L., "F-16 Wing Structure Deflection Testing-Phase I," *U.S. Air Force T&E Days*. AIAA Paper 2007-1674, Feb. 2007.
[22] Sharma, V. and Denegri, C., "F-16 Limit Cycle Oscillation Simulation Using ZONA Euler Unsteady Solver (ZEUS)'" *Aerospace Flutter & Dynamics Council*, 25 October 2012.
[24] Massett, A.P., *AIM-9 Control Surface Effects on Subsonic LCO Analysis for F-16 Store Configuration Clearance*, M.S. Thesis, Air Force Institute of Technology, 2011.
[25] Chen, P.C., Zhang, Z., Zhou, Z., Wang, X.Q., and Mignolet, M.P., "Nonlinear Structural Damping Effects on F-16 Limit Cycle Oscillations," *Proceedings of the AIAA Science and Technology Forum and Exposition (SciTech2018)*, Kissimmee, Florida, Jan. 8-12, 2018, AIAA Paper AIAA-2064.

COPYRIGHT STATEMENT